PAPER

Theoretical understanding of evolutionary dynamics on inhomogeneous networks

To cite this article: Hamid Teimouri *et al* 2023 *Phys. Biol.* **20** 036003

View the article online for updates and enhancements.

Physical Biology

PAPER

Theoretical understanding of evolutionary dynamics on inhomogeneous networks

Hamid Teimouri[1,2] [iD], Dorsa Sattari Khavas[3], Cade Spaulding[5], Christopher Li[4] and Anatoly B Kolomeisky[1,2,3,4,*] [iD]

[1] Department of Chemistry, Rice University, Houston, TX 77005-1892, United States of America
[2] Center for Theoretical Biological Physics, Rice University, Houston, TX 77005-1892, United States of America
[3] Department of Chemical and Biomolecular Engineering, Rice University, Houston, TX 77005-1892, United States of America
[4] Department of Physics and Astronomy, Rice University, Houston, TX 77005-1892, United States of America
[5] Trinity University, San Antonio, TX 78212, United States of America
[*] Author to whom any correspondence should be addressed.

E-mail: tolya@rice.edu

Abstract

Evolution is the main feature of all biological systems that allows populations to change their characteristics over successive generations. A powerful approach to understand evolutionary dynamics is to investigate fixation probabilities and fixation times of novel mutations on networks that mimic biological populations. It is now well established that the structure of such networks can have dramatic effects on evolutionary dynamics. In particular, there are population structures that might amplify the fixation probabilities while simultaneously delaying the fixation events. However, the microscopic origins of such complex evolutionary dynamics remain not well understood. We present here a theoretical investigation of the microscopic mechanisms of mutation fixation processes on inhomogeneous networks. It views evolutionary dynamics as a set of stochastic transitions between discrete states specified by different numbers of mutated cells. By specifically considering star networks, we obtain a comprehensive description of evolutionary dynamics. Our approach allows us to employ physics-inspired free-energy landscape arguments to explain the observed trends in fixation times and fixation probabilities, providing a better microscopic understanding of evolutionary dynamics in complex systems.

1. Introduction

The most unique property of all biological systems is their ability to evolve over time by preferentially selecting randomly appearing features that benefit them most [8, 16]. While the main trends of evolution are now reasonably well understood, many aspects of evolutionary dynamics remain unclarified [8, 20]. In recent years, it was proposed to explore evolutionary dynamics on graphs as a way to mimic evolutionary processes for populations that possess complex structures, for example, as typically found in biological tissues [15, 34]. This approach has been widely utilized for investigating a variety of phenomena ranging from cancer initiation and evolution to social cooperativity and ecological dynamics, providing

new insights into mechanisms of these processes [9, 13, 23, 24, 27–29, 31, 37]. There have been multiple observations confirming that spatial structure of populations might have a strong effect on evolutionary dynamics [2, 4, 9, 14, 17, 21], but there is still no clear understanding of why it is happening.

It is widely accepted that populations evolve following a specific sequence of events [20]. After a random mutation appears in one of the individuals in the population, it might proliferate in the system via selection and random drift, eventually spreading to the whole population in a process known as fixation. But the fixation is not guaranteed, and the mutation might also disappear since the birth-death events in the successive generations are random. Then the most crucial properties to characterize these processes

are a fixation probability, which is defined as the probability for the given mutation to fully occupy the population, and a fixation time, which is defined as the mean time between the first appearance of the given mutation and its final fixation [1, 12, 26, 31, 32, 34, 36]. Because biological systems are typically very inhomogeneous, the fixation processes in these systems have been frequently investigated by exploring methods of evolutionary dynamics on graphs, which led to several remarkable observations [15, 31, 32, 34]. For example, while it was naively expected that homogeneous well-mixed populations exhibit the highest fixation probabilities, several network topologies have been identified expressing even higher fixation probabilities [15, 32, 34]. These systems have been labeled as amplifiers, and it has been suggested that they might accelerate the evolution [15]. However, all these networks amplify the selection of mutations at the cost of significantly slowing down the fixation dynamics, i.e. the fixation times in these systems are always larger than the fixation times for similar-size homogeneous well-mixed populations [33]. Although the fixation processes for inhomogeneous populations have been intensively studied in recent years [3, 5, 6, 18, 19, 25, 32, 34], there is still no clear understanding on the microscopic origin of selection amplifications, the connections to the underlying network topology, and the correlations between the fixation probabilities and the fixation times.

In this paper, we present a theoretical investigation of evolutionary dynamics on inhomogeneous populations by applying a method of stochastic mapping [31], as an alternative to the discrete-time Markov chain method [5]. Our method does not depend on the time update in the system. The main idea is that all evolutionary processes can be viewed as stochastic transitions between discrete states. The time updates only specify how these transitions are taking place. The method works equally well for both continuum-time and discrete-time updates. We chose to utilize a continuous-time description since it provides a more realistic description of natural processes. In our approach, evolutionary changes in the system can be viewed as stochastic transitions between specific discrete states that are identified with different numbers of mutated individuals in the populations. To be more specific, we explicitly analyze evolutionary dynamics on star networks that are known to be selection amplifiers for Birth-Death updating rule [10, 11, 22]. Explicit expressions for fixation probabilities and fixation times are obtained using first-passage probabilities calculations and physically consistent approximations. Similar expressions for fixation probabilities have been derived in [5] using a discrete-time Markov chain description of the underlying dynamics. However, we employ a continuous-time description of stochastic transitions that is more

realistic for biological processes. Theoretical calculations are supported by extensive Monte Carlo computer simulations. It is argued that the overall evolutionary process in the system can be viewed as a motion in the effective free-energy landscape, allowing us to explain the microscopic origin of amplification and the observations of larger fixation probabilities together with slower fixation times.

2. Theoretical method

2.1. Evolutionary dynamics on graphs

Let us investigate a specific biological population that can evolve following random mutations and sequential selection processes. To be specific, we consider an originally healthy tissue with N wild-type stem cells (i.e. those cells that can replicate). At some time (assumed to be $t = 0$), a mutation appears in one of the cells [7, 35]. The tissue cells can replicate, although the rates are different for normal (wild-type) and mutated cells. It is assumed that the division rate for normal cells is equal to b, while the mutated cells dive with a rate $r \times b$. The parameter r is defined here as a fitness parameter that specifies how faster is the replication rate for the mutated cells in comparison with the wild-type cells. It plays a critical role in dynamic processes, since it assists the evolution in choosing the specific mutations to take over the whole tissue [20, 31]. For $r > 1$, the mutations are viewed as advantageous, while for $r < 1$ the mutations are disadvantageous. In addition, $r = 1$ specifies neutral mutations. For convenience, we assume here that the replication rate of normal cells is $b = 1$.

Another crucial factor that drives the evolution is a requirement to have the total number of cells N to be constant [31]. For biological tissues, it is a consequence of homeostasis when the most relevant physiological properties of organisms tend to be constant [16]. Although the specific mechanisms of how the number of cells in the tissues is kept constant at the microscopic level are not yet fully understood, the popular approach to mimic the processes that support homeostasis is to utilize a so-called Moran procedure [20]. Here we adapt a Birth-death updating rule, which is a two-step process in which a new cell is born and then the extra cell is removed. Thus, in Birth-death updating selection is based on birth. First, one of N cells is randomly chosen to replicate proportionally to its fitness ('Birth'). This temporarily increases the number of cells in the tissue to $N + 1$. Then one of $N + 1$ cells is chosen to be instantaneously removed ('Death') to return to the original number of cells in the tissue. Alternatively, one can use a death-Birth update rule, in which selection occurs after death [10, 11]. It is interesting to note that the quantitative results for both updates differ: a Birth-death update makes the star graph an amplifier of natural selection, while a death-Birth update makes the star graph a suppressor of natural selection [10].
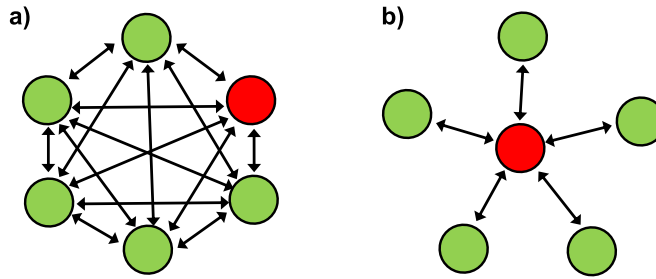
Figure 1. Schematic view of evolutionary dynamics on networks. Arrows indicate allowed changes after the replications. Green cells are normal and red cells are mutated. (a) A homogeneous well-mixed model of size N where the replications at any node can lead to the removal of any other $(N-1)$ cells with equal probability $1/(N-1)$. (b) An inhomogeneous network where the replication at one special star node can affect any other $(N-1)$ cells with probability $1/(N-1)$, while the replications at any of the $(N-1)$ branched cells can only change the star node with unit probability.

One should also notice that our two-step procedure of obtaining transition rates is very convenient to emphasize the differences between two updates in evolutionary dynamics.

To better understand the complex dynamic processes in biological systems, it has been proposed to investigate the evolutionary dynamics on networks [15, 34]. This is schematically illustrated in figure 1. The idea here is that networks efficiently reflect spatial inhomogeneity and variations in activity in the biological tissues. In this approach, each node corresponds to one cell, and connections between nodes specify the direction of selection processes after the replication. The advantage of analyzing the dynamics on graphs is that both homogeneous (figure 1(a)) and inhomogeneous networks (figure 1(b)) can be investigated in one framework, allowing for better understanding of the role of population structures in evolutionary dynamics.

To explain evolutionary processes on graphs, let us first consider the homogeneous network presented in figure 1(a). In this model, there are N identical cells, and the Moran procedure here is the following. After the randomly selected cell replicates, temporary increasing the number of cells to $N+1$, with the probability $1/(N-1)$ any other of $(N-1)$ cells is substituted by the newly created cell, bringing down the number of cells again to N. This is a well-mixed homogeneous system for which the fixation dynamics has been fully investigated [15, 20, 31]. More specifically, the fixation probability for this system is equal to

$$\Pi_1^{(\mathrm{hom})} = \frac{1-1/r}{1-1/r^N},\tag{1}$$

while the fixation time is given by [28],

$$T_1^{(\mathrm{hom})} = (N-1)\sum_{n=1}^{N-1}\frac{1}{n(N-n)}$$
$$\times\left(\frac{r^n-1}{r-1}\right)\left(\frac{r^{N-n}-1}{r^N-1}\right).\tag{2}$$

The sub-index '1' in these expressions corresponds to the fact that the evolutionary process starts with just

one mutated cell, while the super-index hom reflects that the system is homogeneous. In the limit of $r\to 1$ (neutral mutations), the fixation probabilities and fixations times simplify into

$$\Pi_1^{(\mathrm{hom})} = \frac{1}{N},\quad T_1^{(\mathrm{hom})} = \frac{(N-1)^2}{N}.\tag{3}$$

Another important limiting and more realistic case is when $N\to\infty$ for $r>1$. In this case, it can be shown that

$$\Pi_1^{(\mathrm{hom})} \simeq 1-1/r,\quad T_1^{(\mathrm{hom})} \simeq \ln N.\tag{4}$$

2.2. Evolutionary dynamics on star networks

Now let us consider the evolutionary dynamics for inhomogeneous populations. More specifically, we concentrate on the star network as presented in figure 1(b). This is the system where the fixation probability amplifications has been observed [15, 33]. In this model, there are two types of cells: one central node and $(N-1)$ branched nodes. After the replication takes place in the central cell, the selection can substitute any of the branched cells with the probability $1/(N-1)$. However, if the replication occurs at the branched cells, then only the central cell will be substituted with the unit probability.

To investigate the fixation dynamics in the star network, we explore a method of stochastic mapping that has been already successfully utilized for understanding cancer initiation processes [27–29, 31]. The main idea of this approach is to view the evolutionary processes as a set of stochastic transitions between different states. These states are specified by the number of mutated cells. For the star model, this approach is illustrated in figure 2. We define the state $n^{(0)}$ as the one that has n mutated cells, but only in the branched nodes and not in the center, while the state n defines the situation with n mutated cells that includes the central node. Arrows in figure 2 identify possible transitions between the states. There are four types of transition rates. The rate $a_n^{(0)}$ describes the transitions from the state $n^{(0)}$ to the state $n+1$, and the rate a_n describes the transition from the state n to
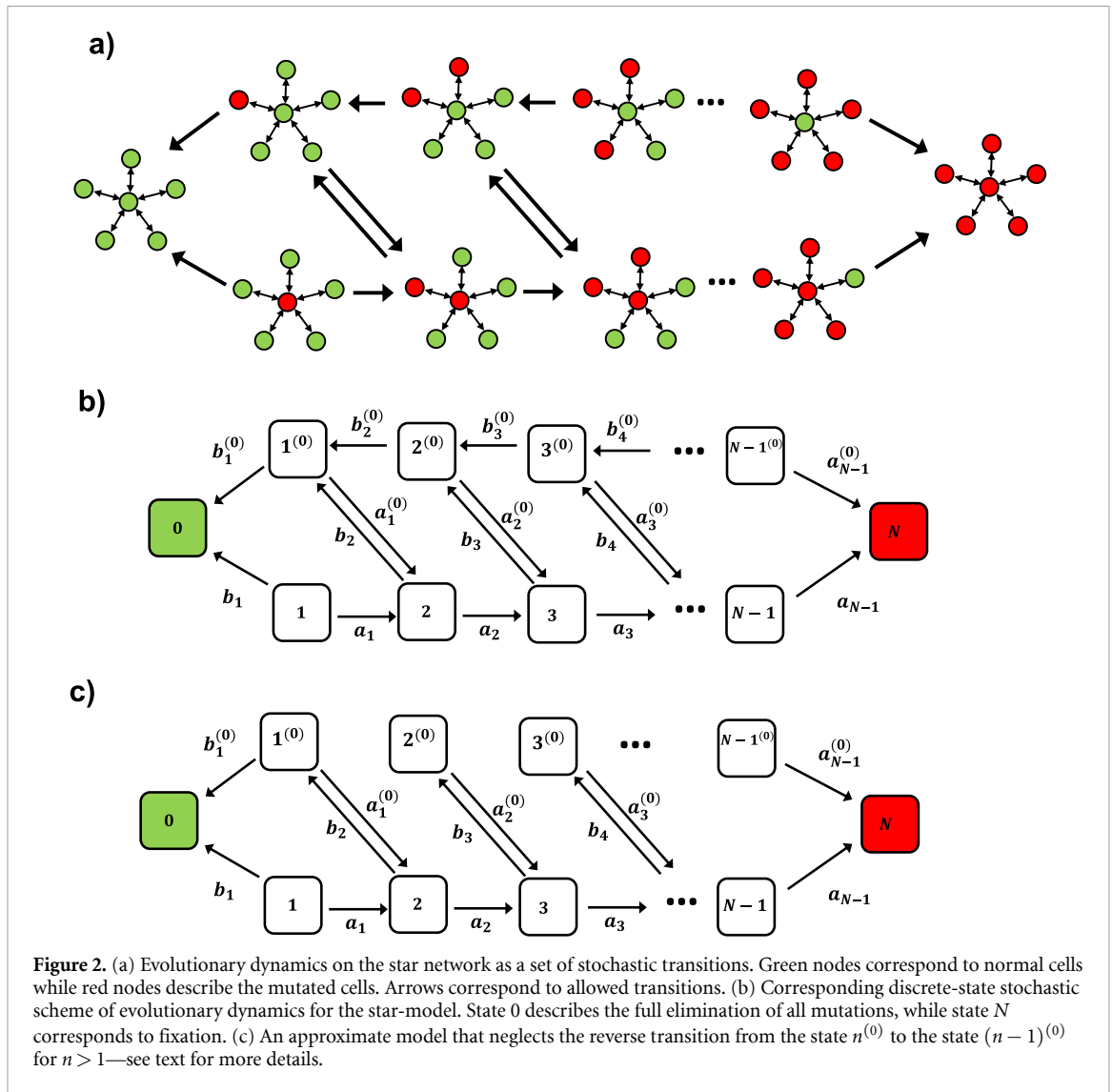
Figure 2. (a) Evolutionary dynamics on the star network as a set of stochastic transitions. Green nodes correspond to normal cells while red nodes describe the mutated cells. Arrows correspond to allowed transitions. (b) Corresponding discrete-state stochastic scheme of evolutionary dynamics for the star-model. State 0 describes the full elimination of all mutations, while state N corresponds to fixation. (c) An approximate model that neglects the reverse transition from the state $n^{(0)}$ to the state $(n-1)^{(0)}$ for $n > 1$—see text for more details.

the state $n+1$ (figure 2(b)). It corresponds to the increase in the number of mutated cells in the system. The decrease in the number of mutated cells are given by the rates $b_n^{(0)}$ ($n^{(0)} \to (n-1)^{(0)}$) and the rates b_n ($n \to (n-1)^{(0)}$): see figure 2(b). Importantly, one can see two types of states between the state without mutations ($n=0$) and the fully mutated state ($n=N$): see figure 2. But effectively only one of them leads to the fixation.

As explained in the supporting information, the specific expressions for the transition rates are given by

$$a_n^{(0)} = nr; \qquad a_n = r\left(\frac{N-n}{N-1}\right); \qquad (5)$$

$$b_n^{(0)} = \frac{n}{N-1}; \qquad b_n = N-n. \qquad (6)$$

This allows us to fully evaluate the fixation dynamics on the star networks. For this purpose, we utilize a method of first-passage probabilities that has been successful in analyzing the mechanisms of cancer

initiation [28, 29, 31]. We define functions $F_n(t)$ [$F_n^{(0)}(t)$] as the probability densities of reaching the fixation state $n = N$ at time t if at $t = 0$ the system started in the state n [$n^{(0)}$]. The time evolution of these probability density functions is governed by the following set of backward master equations,

$$\frac{\mathrm{d}F_n^{(0)}}{\mathrm{d}t} = a_n^{(0)} F_{n+1} + b_n^{(0)} F_{n-1}^{(0)} - (a_n^{(0)} + b_n^{(0)}) F_n^{(0)}, \qquad (7)$$

$$\frac{\mathrm{d}F_n}{\mathrm{d}t} = a_n F_{n+1} + b_n F_{n-1}^{(0)} - (a_n + b_n) F_n, \qquad (8)$$

with initial condition $F_N(t) = \delta(t)$, which means that if the system starts in the state $n = N$ the fixation is immediately accomplished.

From the first-passage probabilities, the details of evolutionary dynamics on star networks can be fully identified. More specifically, one can calculate the fixation probabilities $\pi_n = \int_0^\infty F_n(t)\mathrm{d}t$ and the fixation

times $T_n = \int_0^\infty t F_n(t) \mathrm{d}t / \pi_n$. As shown in the supporting information, the fixation probabilities starting from the states n or $n^{(0)}$ are given by,

$$\Pi_n^{(0)} = \frac{1 + \frac{1}{r(N-1)} - \left(\frac{1}{r^2} + \frac{1}{r(N-1)} \right)^n}{\left[1 + \frac{1}{r(N-1)} \right] \left[1 - \frac{1}{r^2} \left(\frac{1 + \frac{N-1}{r}}{1 + r(N-1)} \right)^{N-2} \right]}; \quad (9)$$

and

$$\Pi_n = \frac{1 - \frac{1}{r^2} \left(\frac{1 + \frac{N-1}{r}}{1 + r(N-1)} \right)^{n-2}}{\left[1 - \frac{1}{r^2} \left(\frac{1 + \frac{N-1}{r}}{1 + r(N-1)} \right)^{N-2} \right]}. \quad (10)$$

Interestingly, it can be shown that generally for all values of n we have $\Pi_n^{(0)} > \Pi_n$. If starting from the single-mutation states ($n = 1$), the fixation probabilities are equal to

$$\Pi_1^{(0)} = \frac{1 - \frac{1}{r^2}}{\left[1 + \frac{1}{r(N-1)} \right] \left[1 - \frac{1}{r^2} \left(\frac{1 + \frac{N-1}{r}}{1 + r(N-1)} \right)^{N-2} \right]}; \quad (11)$$

$$\Pi_1 = \frac{1 - \frac{1}{r^2}}{\left[1 + \frac{N-1}{r} \right] \left[1 - \frac{1}{r^2} \left(\frac{1 + \frac{N-1}{r}}{1 + r(N-1)} \right)^{N-2} \right]}. \quad (12)$$

To better understand the microscopic picture of fixation processes, it is useful to consider limiting situations. If the replication rates of mutated cells are the same as for the normal cells ($r = 1$, neutral mutations), from equation (11) we obtain

$$\Pi_1^{(0)} = \frac{N-1}{N + (N-1)(N-2)};$$
$$\Pi_1 = \frac{1}{N + (N-1)(N-2)}. \quad (13)$$

which for large number of cells ($N \gg 1$) simplify into

$$\Pi_1^{(0)} \simeq \frac{1}{N}; \quad \Pi_1 \simeq \frac{1}{N^2}. \quad (14)$$

Another important limit is when $r > 1$ and $N \to \infty$. In this case, it can be shown that

$$\Pi_n^{(0)} = \frac{1 - \frac{1}{r^{2n}}}{1 - \frac{1}{r^{2N}}} \simeq 1 - \frac{1}{r^{2n}},$$

$$\Pi_n = \frac{1 - \frac{1}{r^{2n-2}}}{1 - \frac{1}{r^{2N-2}}} \simeq 1 - \frac{1}{r^{2n-2}}. \quad (15)$$

Starting from the single-mutation states ($n = 1$), these calculations yield

$$\Pi_1^{(0)} = \frac{1 - \frac{1}{r^2}}{1 - \frac{1}{r^{2N}}} \simeq 1 - \frac{1}{r^2}, \quad \Pi_1 = \frac{1 - \frac{1}{r^{2-2}}}{1 - \frac{1}{r^{2N-2}}} \simeq 0. \quad (16)$$

It is important to note that the asymptotic result for $\Pi_1^{(0)}$ was originally derived in [15] as an approximate form for fixation probability for large N. When the mutation appears first in one of the branched cells (starting in the state $1^{(0)}$) our limiting results fully agree with previous calculations for the fixation probability in star networks [15]. But starting in the center of the network (the state 1) does not essentially lead to the fixation at all for the large N.

The results of our calculations are presented in figure 3. As it was shown in [28] (see also equation (4)), for very large N, the fixation probability for the well-mixed Moran model behaves as $\Pi_1^{(\mathrm{hom})} \simeq \frac{1}{1 - 1/r}$. Then, using equation (16), the asymptotic value of the ratio of fixation probabilities (green curve in figure 3(a)) is given by

$$\frac{\Pi_1^{(0)}}{\Pi_1^{(\mathrm{hom})}} = \frac{1 - \frac{1}{r^2}}{1 - \frac{1}{r}} \simeq 1 + \frac{1}{r}, \quad (17)$$

which in the limit of $r \to 1$ approaches 2, as illustrated in figure 3(b). The most interesting observation here is that the fixation probability strongly depends on which initial cell is mutated. The mutation in one of the branched states leads to the amplification of fixation probabilities, while the mutation in the center node of the network significantly decreases the probability of fixation: see figure 3. Our theoretical approach allows us to clearly understand these observations. From the discrete-state stochastic scheme in figure 2(b), one might conclude that the main pathway of eliminating the mutation from the state $1^{(0)}$ to go directly to the state 0, and its probability is given by

$$P_{1^{(0)}}(\text{elimination}) = \frac{b_1^{(0)}}{b_1^{(0)} + a_1^{(0)}} = \frac{1}{1 + r(N-1)}, \quad (18)$$

which in the limit $N \to \infty$ approaches zero. It is important to notice here that we consider here only neutral or beneficiary mutations ($r \geqslant 1$). The probability of eliminating the mutation from the state 1 is equal to

$$P_1(\text{elimination}) = \frac{b_1}{b_1 + a_1} = \frac{N-1}{r + (N-1)}, \quad (19)$$

which in the limit $N \to \infty$ approaches unity. Since the fixation is opposite to the mutation elimination $[\Pi_j \approx 1 - P_j(\text{elimination})$ in this limit], one can see that it is more probable to remove the mutation from the central cell, while it is much less probable to eliminate the mutation from the branched cell. This is the origin of the fixation amplification phenomenon in the star networks.

The results presented in figure 3(b) also suggest that the highest degree of amplification $(\Pi_1^{(0)}/\Pi_1^{(\mathrm{hom})})$ generally cannot be larger than two,
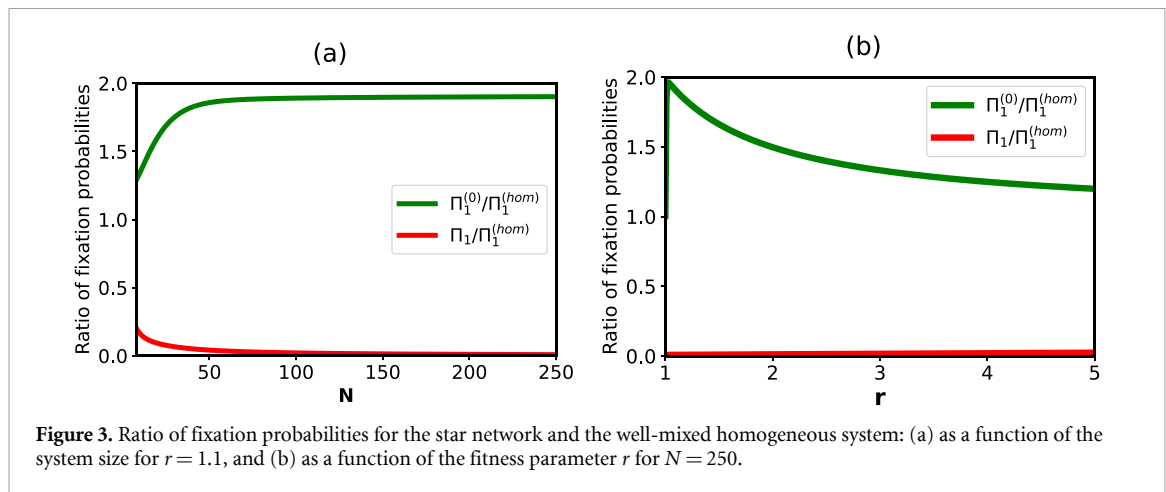
Figure 3. Ratio of fixation probabilities for the star network and the well-mixed homogeneous system: (a) as a function of the system size for $r = 1.1$, and (b) as a function of the fitness parameter r for $N = 250$.

and it can be achieved only for the fitness parameters that are only slightly larger than one. This is one of the main results of our investigation. Interestingly, for neutral mutations ($r = 1$), the theoretical calculations predict that there will be no amplification at all ($\Pi_1^{(0)}/\Pi_1^{(hom)} = 1$), and this has been also observed before. This is a consequence of the behavior of fixation probabilities at $r = 1$ and large N, namely $\Pi_1^{(0)} \approx \Pi_1^{(hom)} \simeq 1/N$. Thus, the fixation amplification works well only for slightly advantageous mutations.

Another interesting observation from our theoretical analysis is the dependence of the degree of amplification on the system size (figure 3(a)) and the fitness parameter r (figure 3(b)). Increasing the number of cells in the tissue makes the amplification stronger. This is because the probability of mutation elimination from the state $1^{(0)}$ behaves as $1/N$. Surprisingly, making the mutation more advantageous (larger r) lowers the degree of amplification—see figure 3(b). It can be shown that $\Pi_1^{(0)}/\Pi^{(hom)} \simeq 1 + 1/r$ for large number of cells. This can be explained by arguing that there are more pathways to reach the fixation in the well-mixed homogeneous system, while it is only one pathway in the star-network model. Then, larger fitness parameters r increase the fixation probability more for the homogeneous system than for the inhomogeneous system.
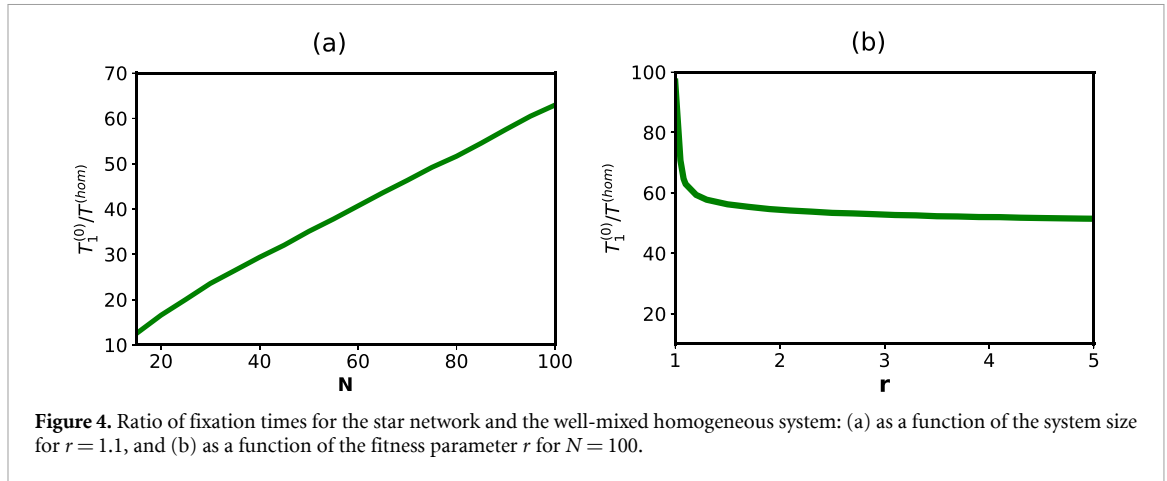
While we were not able to obtain explicit expressions for the fixation times, they can be evaluated numerically by solving the corresponding backward master equations, as shown in the supporting information. In addition, we also run Monte Carlo computer simulations to evaluate the fixation dynamics in the star networks. The results of our numerical calculations and computer simulations are presented in figure 4 and compared with the homogeneous well-mixed model. Only the fixation times from the state $1^{(0)}$ are presented there because they are essentially the same as the fixation times starting from the state 1.

One can see that the ratio of fixation times grows linearly with the size of the system (figure 4(a)), suggesting that for $N \gg 1$ the fixation time on the star network scales as $T_{1^{(0)}} \sim N \ln N$. This can be explained in terms of our method of stochastic mapping. In the inhomogeneous star model there is one pathway that leads to the fixation—the one when the center cell is always mutated. However, in the well-mixed homogeneous system there are N such pathways that lead to the fixation since there are no topological constraints there. Figure 4(b) shows that increasing the fitness advantage of the mutated cells accelerates the fixation dynamics in the star network, but the effect is rather modest. We also found that the slowest fixation dynamics is observed for very slightly advantageous mutations where the fixation amplification is the strongest.

Our discrete-state stochastic description allows us to better understand the microscopic mechanisms of evolutionary processes on star networks. It shows that the amplification of the fixation probability is taking place not due to increased number of pathways to reach the fixation state but by lowering the probability of mutation elimination from the branched cells. However, it cannot lead to faster fixation dynamics because the system is frequently trapped in the states where the central node is not mutated (see figure 2(a)), slowing the overall fixation dynamics. In addition, the topology of the network dictates that there is only one pathway to reach the fixation state, while there are many more opportunities in the well-mixed homogeneous systems of the same size to reach the fixation state.

2.3. Approximate model to describe evolutionary dynamics on star networks

To better illustrate the idea of slowing the fixation dynamics in the star network due to trapping the system in the unproductive states, we propose considering an approximate model that captures main features

Figure 4. Ratio of fixation times for the star network and the well-mixed homogeneous system: (a) as a function of the system size for $r = 1.1$, and (b) as a function of the fitness parameter r for $N = 100$.

of the evolutionary dynamics on star networks and allows us to obtain the explicit expressions for the fixation probabilities and fixation times. Our idea here is based on the observation that the probability to move from the state $n^{(0)}$ to the state $(n-1)^{(0)}$ is given by

$$p[n^{(0)} \to (n-1)^{(0)}] = \frac{b_n^{(0)}}{a_n^{(0)} + b_n^{(0)}}$$
$$= \frac{1}{r(N-1)+1} \to 0, \quad (20)$$

for $N \gg 1$. Then it seems reasonable to neglect such transitions and to consider an effective discrete-state stochastic scheme as shown in figure 2(c). Thus, we assume that $b_n^{(0)} \approx 0$ for $n \geqslant 2$, and only the backward transition from the state $1^{(0)}$ is assumed to be non-zero ($b_1^0 \neq 0$).

The fixation dynamics in the approximate model can be explicitly analyzed as shown in the supporting information. More specifically, for fixation probabilities, it is found that

$$\Pi_{1^{(0)}}^{(\text{approx})} = \frac{1}{1 + \frac{1}{r^2} + \frac{1}{r(N-1)}} \simeq \frac{1}{1 + \frac{1}{r^2}}; \quad (21)$$

$$\Pi_1^{(\text{approx})} = \frac{1}{1 + \frac{N-1}{r}} \simeq 0; \quad (22)$$

$$\Pi_2^{(\text{approx})} = \frac{1 + \frac{1}{r(N-1)}}{1 + \frac{1}{r^2} + \frac{1}{r(N-1)}} \simeq \frac{1}{1 + \frac{1}{r^2}}. \quad (23)$$

In addition, $\Pi_n^{(\text{approx})} = 1$ for $n \geqslant 3$ and $\Pi_{n^{(0)}}^{(\text{approx})} = 1$ for $n \geqslant 2$. Figure 5 compares the predictions for the fixation probabilities for the approximate model of evolutionary dynamics. One can see that our approximation works quite well when $r^2 \gg 1$, and increasing the size of the system only slightly improves the agreement (figure 5(a)). But in all situations, the difference is only few percents between exact and approximate estimates of the fixation probabilities. At the same time, increasing the fitness parameter of the mutated cells has a much stronger effect (figure 5(b)).

This is because the relation on which our approximation is based, equation (20), works even better for larger fitness parameters r. In all cases, we overestimate the fixation probabilities in comparison with exact expressions. This can be easily understood by again exploring the stochastic schemes in figures 2(b) and (c). One can clearly see that our approximate model neglects the occasional backward steps in the upper chain of states that should only lower the fixation probability, in agreement with our predictions. These observations also suggest that our approximation works only qualitatively in the regime of maximal amplification when r is very close to unity, but still it allows us to clarify better some general microscopic aspects of evolutionary dynamics.

As shown in the supporting information, we can obtain the explicit expressions for the fixation times of the approximate model. It is found that

$$T_n^{(\text{approx})} = \sum_{k=0}^{N-n-1} \frac{a_{n-1+k}^{(0)} + b_{n+k}}{a_{n+k} a_{n-1+k}^{(0)}}, \quad (24)$$

for $n \geqslant 3$. In the limit $N \to \infty$, it can be shown that $T_{1^{(0)}}^{(\text{approx})} \simeq T_3^{(\text{approx})}$ that eventually leads to the following estimate of the fixation time,

$$T_{1^{(0)}}^{(\text{approx})} \simeq \frac{(N-1)}{r^2} \left(\sum_{k=2}^{N-2} \frac{1}{k} + \sum_{k=2}^{N-2} \frac{r}{N-k-1} \right)$$
$$\simeq \frac{(r+1)}{r^2} N \ln N. \quad (25)$$

Thus, the approximate model correctly reproduces the scaling dependence of the fixation time [34].

Theoretical predictions for the fixation dynamics in the approximate and full models of evolutionary dynamics on star networks are presented in figure 6. One can see from figure 6(a) that approximating the fixation times is reasonable, although not as good as approximating the fixation probabilities: deviation of $\sim 20\%$ for times in comparison with $\sim 5\%$ for the probabilities for $r = 2$ case. The increasing the size of the system also does not have much effect. At the same time, increasing the advantage of the mutated cells
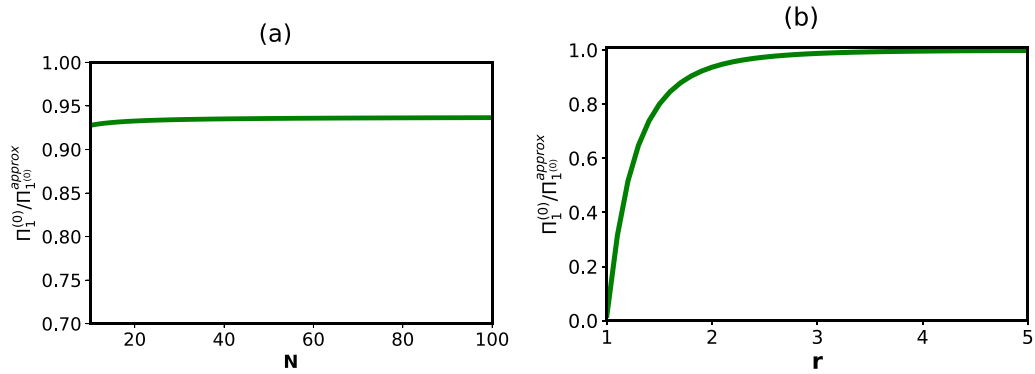
Figure 5. Comparison of fixation probabilities for the approximate and full models of evolutionary dynamics on star networks. Ratio of fixation probabilities (a) as a function of the system size for $r = 2$, and (b) as a function of the fitness parameter r for $N = 100$.
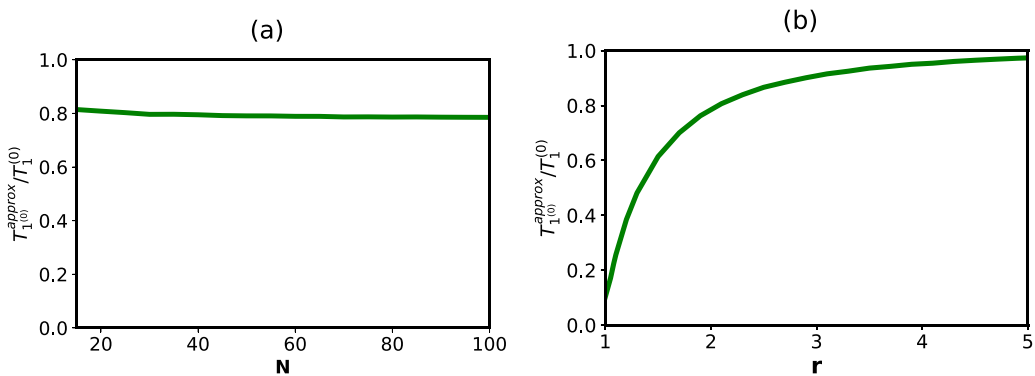

Figure 6. Comparison of fixation times for the approximate and full models of evolutionary dynamics on star networks. Ratio of fixation times (a) as a function of the system size for $r = 2$, and (b) as a function of the fitness parameter r for $N = 100$.

(larger values of r) significantly improves the approximation: see figure 6(b). As before, these observations can be understood by utilizing the discrete-state stochastic schemes from figure 2. Because the approximate model neglects the backward transitions from the states $n^{(0)}$, it underestimates the fixation times by neglecting the backward and loop trajectories that should significantly slow down the overall dynamics in the system.

Although the approximate model does not perfectly describe the fixation dynamics on the star network, it is valuable because it emphasizes better the main features of the evolutionary processes in these complex systems. The fixation amplification occurs only because the topological features of the system prevent the mutation elimination, while the fixation dynamics is quite slow because the system is frequently trapped in the unproductive states that are not on the pathway to the fixation. It is important to point out that this clear microscopic picture emerges as the result of mapping the evolutionary dynamics into the set of stochastic transitions between states specified by different numbers of mutated cells.

Another advantage of our discrete-state stochastic approach is that looking at the evolutionary processes as a motion in the effective free-energy landscape allows us to describe better the microscopic mechanisms of underlying processes and to discuss possible ways to optimize the evolution. This is schematically shown in figure 7. The fixation probability might be associated with the 'free-energy' difference between the final state (fixation) and the initial state (one mutated cell), while the fixation times are given by the highest barrier on the pathway from the initial to the final states. For the well-mixed homogeneous system, the advantage of reaching the fixation state is relatively modest, but the dynamics is also relatively fast. The situation is completely different for the evolutionary dynamics on the star network: see figure 7. Here, the advantage of reaching the fixation state is significant, but the 'free-energy' barrier to accomplish this task is also quite large. As was discussed above, it is the consequence of the topological properties of the star network. Thus, to accelerate the evolution, changes must be made to decrease these barriers and not in trying to increase the amplification of fixation probabilities. Our theoretical method suggests that one can concentrate on specific discrete states where such changes will be the most effective.

To be more specific, one can utilize a quantitative approach that we recently developed to connect effective free energies and transitional rates [30].
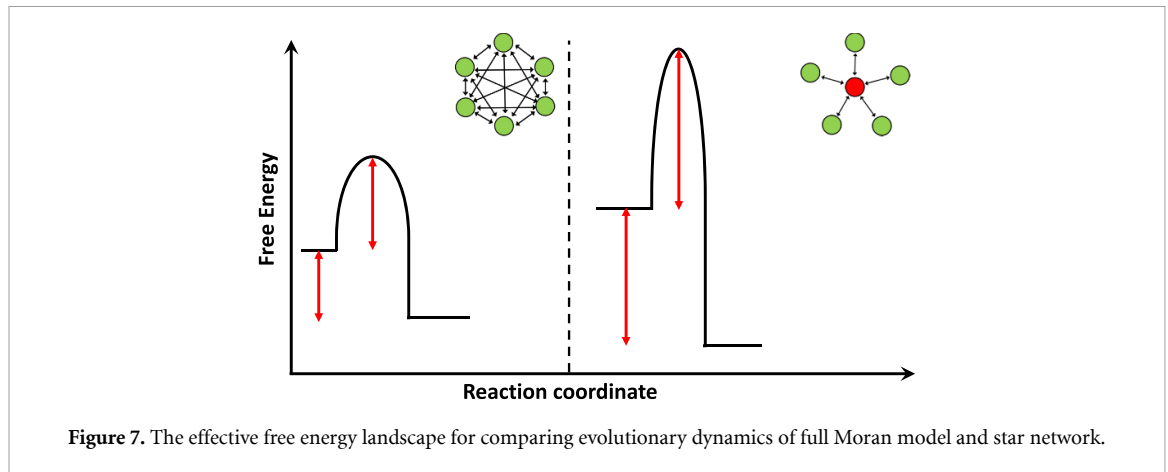
Figure 7. The effective free energy landscape for comparing evolutionary dynamics of full Moran model and star network.

According to this method, one can assume that the effective free energy at the state j is connected with the residence time at the state j, τ_j,

$$G_{\text{eff},j} \simeq \ln(1/\tau_j), \qquad (26)$$

where

$$\tau_n^{(0)} = \frac{1}{a_n^{(0)} + b_n^{(0)}}, \quad \tau_n = \frac{1}{a_n + b_n}. \qquad (27)$$

This means that the shorter the residence time, the higher the effective free energy at the given state. Then, using the explicit expressions for transition rates from equations (5) and (6), one might conclude that the highest free energy on the pathway to the fixation is in the state $n = 2$. Thus, our analysis suggests that the biggest barrier in the evolutionary dynamics is to move from the state $1^{(0)}$ to the state $n = 3$ via the state $n = 2$. This knowledge might help in designing networks with more efficient fixation dynamics.

3. Summary and conclusions

In this paper, we developed a theoretical framework to investigate the role of inhomogeneity in evolutionary dynamics of structured populations. By analyzing the mutation fixation processes on the star network, we constructed a discrete-state stochastic model that provides a comprehensive description of the dynamics. Using the method of first-passage probabilities together with reasonable approximations explicit expressions for the fixation probabilities and fixation times are obtained. The presented theoretical method allowed us to better understand the microscopic origin of fixation amplification that is accompanied by significant increase in fixation times. It is argued that the amplification is the result of decreasing the probability of mutation elimination, but it does not increase the number of pathways to reach the fixation state, leading to slowing down in the fixation dynamics. The mapping of evolutionary dynamics on inhomogeneous networks into the motion in the effective free-energy landscape

provides new insights on the mechanisms of these complex processes. It also suggests how these systems can be modified to optimize the evolutionary output.

The important advantage of our theoretical approach is that the method can be extended for studying the evolutionary processes on other inhomogeneous systems. Specifically, we plan to generalize our theoretical arguments for analyzing the evolutionary dynamics on l-star networks where there are l star nodes that are connected with all $N - l$ branched cells. The system considered in this paper is a special case with $l = 1$. It will be important to understand how the degree of amplification in those systems correlates with the fixation times. In addition, our theoretical method can be extended for dynamic networks where topological features might fluctuate between several different arrangements. It will be also important to apply these theoretical results for understanding cancer initiation and tumor formation.

Data availability statement

All data that support the findings of this study are included within the article (and any supplementary files).

Author contributions

H T and A B K designed the research; H T, C L, D S K and C S performed the research; H T, C L and A B K wrote the manuscript.

Conflict of interest

We declare that we have no competing interests.

Funding statement

Data accessibility

This article has no additional data.

ORCID iDs

Hamid Teimouri ⓘ https://orcid.org/0000-0002-3319-1187

Anatoly B Kolomeisky ⓘ https://orcid.org/0000-0001-5677-6690

References

[1] Allen B, Sample C, Steinhagen P, Shapiro J, King M, Hedspeth T, Goncalves M and Traulsen A 2021 Fixation probabilities in graph-structured populations under weak selection *PLoS Comput. Biol.* **17** e1008695

[2] Antal T, Redner S and Sood V 2006 Evolutionary dynamics on degree-heterogeneous graphs *Phys. Rev. Lett.* **96** 188104

[3] Askari M and Aghababaei Samani K A 2015 Analytical calculation of average fixation time in evolutionary graphs *Phys. Rev.* E **92** 042707

[4] Bozic I and Nowak M A 2013 Unwanted evolution *Science* **342** 938–9

[5] Broom M and Rychtář J 2008 An analysis of the fixation probability of a mutant on special classes of non-directed graphs *Proc. R. Soc.* A **464** 2609–27

[6] Frean M, Rainey P B and Traulsen A 2013 The effect of population structure on the rate of evolution *Proc. R. Soc.* B **280** 20130211

[7] Hanahan D and Weinberg R A 2011 Hallmarks of cancer: the next generation *Cell* **144** 646–74

[8] Heams T, Huneman P and Lecointre G 2015 Marc silberstein and fondateur deséditions matériologiques *Handbook of Evolutionary Thinking in the Sciences* (Berlin: Springer)

[9] Hindersin L and Traulsen A 2014 Counterintuitive properties of the fixation time in network-structured populations *J. R. Soc. Interface* **11** 20140606

[10] Hindersin L, Traulsen A and Komarova N L 2015 Most undirected random graphs are amplifiers of selection for birth-death dynamics, but suppressors of selection for death-birth dynamics *PLoS Comput. Biol.* **11** e1004437

[11] Kaveh K, Komarova N L and Kohandel M 2015 The duality of spatial death–birth and birth–death processes and limitations of the isothermal theorem *R. Soc. Open Sci.* **2** 140465

[12] Kimura M and Ohta T 1969 The average number of generations until fixation of a mutant gene in a finite population *Genetics* **61** 763

[13] Koldaeva A, Tsai H-F, Shen A Q and Pigolotti S 2022 Population genetics in microchannels *Proc. Natl Acad. Sci.* **119** e2120821119

[14] Komarova N L and Myint P C 2006 Epithelial tissue architecture protects against cancer *Math. Biosci.* **200** 90–117

[15] Lieberman E, Hauert C and Nowak M A 2005 Evolutionary dynamics on graphs *Nature* **433** 312–6

[16] Lodish H *et al* 2008 *Molecular Cell Biology* (London: Macmillan)

[17] Marrec Lıc, Lamberti I and Bitbol A-F 2021 Toward a universal model for spatially structured populations *Phys. Rev. Lett.* **127** 218102

[18] Möller M, Hindersin L and Traulsen A 2019 Exploring and mapping the universe of evolutionary graphs identifies structural properties affecting fixation probability and time *Commun. Biol.* **2** 1–9

[19] Monk T and van Schaik Ae 2022 Martingales and the fixation time of evolutionary graphs with arbitrary dimensionality *R. Soc. Open Sci.* **9** 220011

[20] Nowak M A 2006 *Evolutionary Dynamics: Exploring the Equations of Life* (Cambridge, MA: Harvard university press)

[21] Nowak M A, Michor F and Iwasa Y 2003 The linear process of somatic evolution *Proc. Natl Acad. Sci.* **100** 14966–9

[22] Pattni K, Broom M, Rychtář J and Silvers L J 2015 Evolutionary graph theory revisited: when is an evolutionary process equivalent to the moran process? *Proc. R. Soc.* A **471** 20150334

[23] Schimit P H T, Pereira F H and Broom M 2022 Good predictors for the fixation probability on complex networks of multi-player games using territorial interactions *Ecological Complexity* **51** 101017

[24] Seferbekova Z, Lomakin A, Yates L R and Gerstung M 2022 Spatial biology of cancer evolution *Nat. Rev. Genet.* 1–19

[25] Sharma N and Traulsen A 2022 Suppressors of fixation can increase average fitness beyond amplifiers of selection *Proc. Natl Acad. Sci.* **119** e2205424119

[26] Slatkin M 1981 Fixation probabilities and fixation times in a subdivided population *Evolution* **35** 477–88

[27] Spaulding C, Teimouri H and Kolomeisky A B 2022 The role of spatial structures of tissues in cancer initiation dynamics *Phys. Biol.* **19** 056003

[28] Teimouri H, Kochugaeva M P and Kolomeisky A B 2019 Elucidating the correlations between cancer initiation times and lifetime cancer risks *Sci. Rep.* **9** 1–8

[29] Teimouri H and Kolomeisky A B 2021 Temporal order of mutations influences cancer initiation dynamics *Phys. Biol.* **18** 056002

[30] Teimouri H, Spaulding C and Kolomeisky A B 2022 Optimal pathways control fixation of multiple mutations during cancer initiation *Biophys. J.* **121** 3698–705

[31] Teimouri H D and Boris Kolomeisky A B 2022 Can we understand the mechanisms of tumor formation by analyzing dynamics of cancer initiation? *Europhys. Lett.* **137** 27001

[32] Tkadlec J, Pavlogiannis A, Chatterjee K and Nowak M A 2019 Population structure determines the tradeoff between fixation probability and fixation time *Commun. Biol.* **2** 1–8

[33] Tkadlec J, Pavlogiannis A, Chatterjee K, Nowak M A and Traulsen A 2020 Limits on amplifiers of natural selection under death-birth updating *PLoS Comput. Biol.* **16** e1007494

[34] Tkadlec J, Pavlogiannis A, Chatterjee K and Nowak M A 2021 Fast and strong amplifiers of natural selection *Nat. Commun.* **12** 1–6

[35] Weinberg R A 2013 *The Biology of Cancer* (New York: Garland Science)

[36] Whitlock M C 2003 Fixation probability and time in subdivided populations *Genetics* **164** 767–79

[37] Wodarz D and Komarova N 2014 *Dynamics of Cancer: Mathematical Foundations of Oncology* (Singapore: World Scientific)